PII S0008-(98)00261-5

MODELING OF INDUCED MECHANICAL EFFECTS OF ALKALI-AGGREGATE REACTIONS

B. Capra* and J.-P. Bournazel[1]†
*Laboratoire de Génie Civil et Urbanisme, U.F. Génie Civil et Ville, Cité Descartes, 2,
rue A. Einstein, 77420 Champs sur Marne France
†Laboratoire d'Etudes et de Recherches sur les Matériaux, 23, rue de la Madeleine, BP
136–13631 Arles Cedex France

ABSTRACT

Alkali-aggregate reactions (AAR)-induced effects are difficult to model due to the random distribution of the reactive sites and the imperfect knowledge of these chemical reactions. A new approach using fracture mechanics and probabilities and capable of describing the anisotropic swelling of a structure subjected to alkali-silica reaction is presented. © *1998 Elsevier Science Ltd*

Introduction

There is a large number of structures, built more than fifty years ago, which are suffering from deteriorations induced by alkali-aggregate reaction (AAR) that impair durability and might also affect the safety of installations. AAR induces concrete expansions and generally leads to loss of strength and cracking. Presently, there is an increasing interest in the structural response due to AAR effects. The needs and nature of potential interventions must be supported by the knowledge of the spatial distribution and intensity of swelling, the stress state resulting from it, and long term evaluation of the swelling process. Fictitious thermal loading conditions are generally used to reproduce the state of deformations and stresses in a dam. This technique has severe limits. The aim of this paper is to present a new phenomenological modelling capable of describing the AAR induced effects in concrete structures.

Chemical Aspects of the Reactions

AAR are autogeneous chemical reactions. The particularity of these reactions is that they occur inhomogeneously, so only local sites are involved. A lot of work has been done on this chemical reaction and, even if we still do not know exactly all the reactional mechanisms, there are some initial conditions which are required for the beginning of the reactions: some reactive aggregates, alkalis, and sufficient moisture.

---

[1]To whom correspondence should be addressed.

A lot of theories about the mechanisms of these reactions have been published. Nevertheless, for the alkali-silica reaction (ASR), the approach proposed by Glasser and Kataoka (1) seems to be the more realistic. The chemical reactions are assumed to be a two-step phenomenon:

1. Attack of the silanol groups of the reactive silica by the hydroxyl ions
2. Attack of the siloxans bridges of the silica by the hydroxyls ion

The reactions lead to the destruction of the mineral structure of silica and creation of a silico-alkaline gel. This model has been illustrated in (1). The gel composition is very far from being homogenous from one reactive site to another; it depends on numerous factors like time, the initial content of silica, and alkalis. It is also very difficult to talk about one type of gel, even in the same sample of concrete because of the random distribution of the two last previous parameters in the material. During the creation of gel, there is an absorption of water that leads to a swelling. Structural effects depend on the gel swelling. According to (1), a swelling reactive aggregate exerts pressure over the surrounding matrix. The gel created starts to apply pressure when all the surrounding pores are filled. A new production of gel leads to pressures that can be high enough to exceed the tensile strength of the material. Then, cracks arise and, as soon as they open, are filled by the gel. This shows that there is a difference between reaction and expansion: there could be a reaction (production of gel) without swelling of the material (if all the pores are not filled).

A Global Modeling of the AAR

In order to allow structural computations, a global approach has to be used. By a chemical study of the reactions, and from a phenomenological point of view, the principal parameters taken into account are a representative parameter of the chemical reactions (A), temperature (T), and relative humidity (H). Furthermore, from a structural point of view, the function of the stress (σ) is far from being explained. Thus, we can express the AAR free expansion by Eq. 1, and the influence of each parameter is considered in the next paragraphs:

$$\varepsilon^{aar} = \varepsilon^{aar}(A,T,H,\sigma) \qquad (1)$$

Relation Reaction/Expansion

Curves, published by Diamond et al. (2) and presented in Figure 1. show the expansion evolution with time for two temperatures and the percentage of alkalis reacted with time. The idea was to plot, for the two temperatures, the expansion vs. the alkalis reacted. The result is shown in Figure 2.

We can see that temperature has little influence on the curve shape. In order to model the kinetics of reaction, we suppose that the quantity of alkalis reacted is a variable representative of the evolution of the reaction. We have seen previously that expansion and reaction are dissociated: there is expansion when the available voids near the reactive sites are filled by the gel. We suppose that the percentage of alkalis reacted is the representative global parameter of the chemical evolution of the reactions (A). The relation between expansion (ε^{aar}) and alkalis reacted (A) is modelled by a bi-linear law:

Expansion (%)   Percent of alkalis reacted
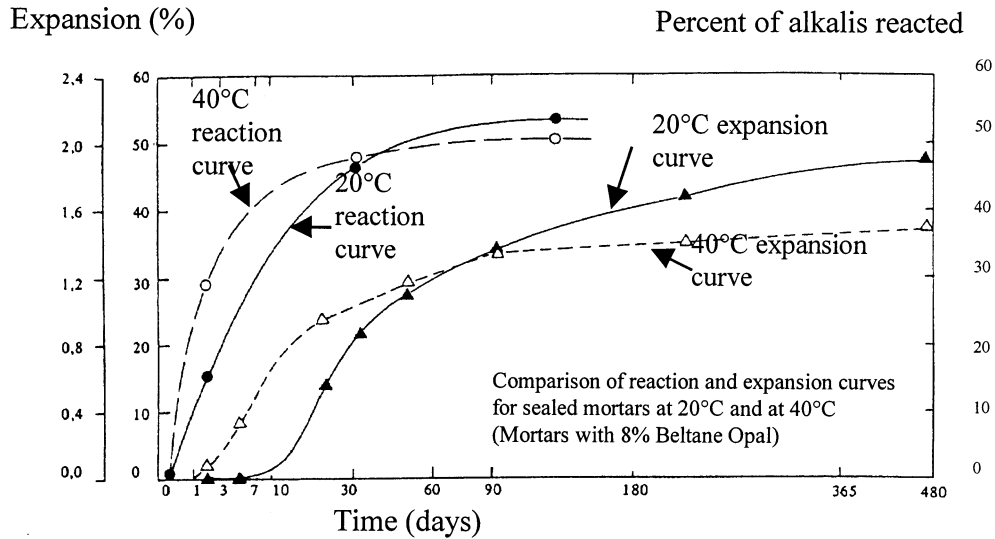

FIG. 1.
Evolution of strains and alkalis reacted for two temperatures (2).

$$\text{for } A \ < \ A_0 : \varepsilon^{\text{aar}} = 0 \tag{2}$$

$$\text{for } A \ > \ A_0 : \varepsilon^{\text{aar}} = \frac{\varepsilon_0}{A_0} \cdot (A \ - \ A_0) \tag{3}$$

where ε_0 and A_0 are defined in Figure 3. The real curve is the curve from Figure 2, A_0 and ε_0 are dependent on concrete material properties such as porosity.

   We shall now introduce a relation between A and time. This relation represents the kinetics of the reaction. After numerous simulations, it has been found that a first-order reaction provides the best results. Thus, we postulate that AAR follows a first-order kinetic law described by:

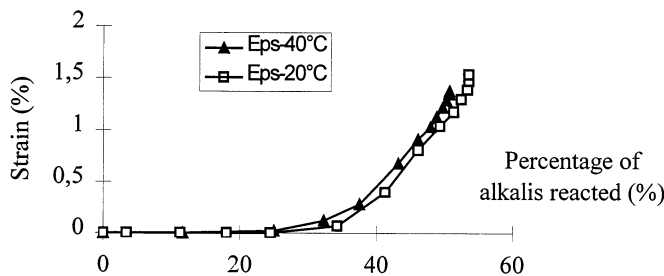$$\frac{dA}{dt} \ = \ k(T) \cdot (1 - A) \tag{4}$$

FIG. 2.
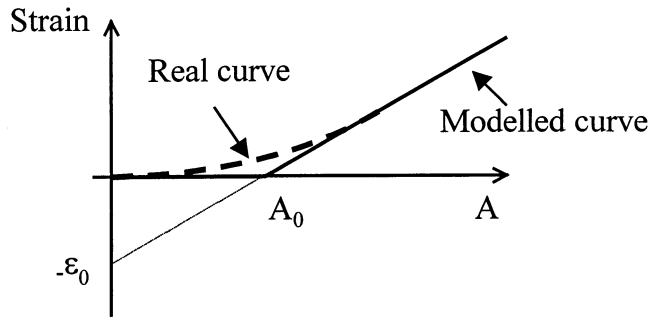Evolution of strain vs. alkalis reacted in the case of mortar bars containing opal.

FIG. 3.
Determination of the parameters.

where $k(T) = k_0 \cdot e^{-E_a/RT}$ is the kinetic constant following the Arrhenius' law (k_0 is the kinetic constant, E_a the activation energy, R the perfect gas constant, and T the temperature). Therefore, the rate of the reaction can be expressed by:

$$A = (1 - e^{-kt}) \tag{5}$$

Finally, the evolution of the expansion related to the reactivity potential takes the form:

$$\varepsilon^{aar}(t,T) = \frac{\varepsilon_0}{A_0} \cdot (1 - A_0 - e^{-k_0 \cdot e^{-\frac{E_a}{RT} \cdot t}}) \quad \text{if } A > A_0 \tag{6}$$

$$\varepsilon^{aar}(t,T) = 0 \qquad\qquad\qquad \text{if } A < A_0 \tag{7}$$

This modeling leads to evolutions shown in Figure 4, which are in substantial agreement with experimental points coming from our experiments.

Relation Humidity/Expansion

The moisture distribution in concrete is very important in determining the reactions. Poole (3) published a curve showing the evolution of the expansion vs. the relative humidity (RH).
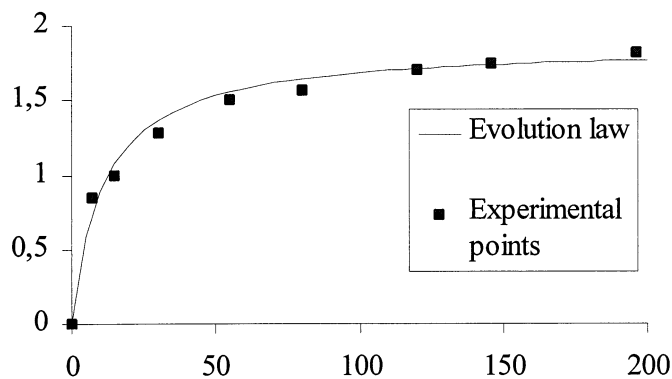

FIG. 4.
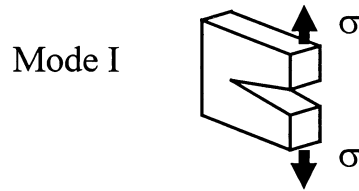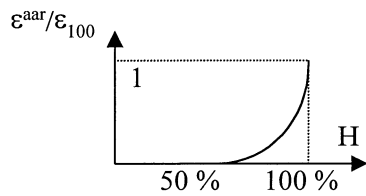Comparison between modeling and experimental curves.

FIG. 5.
Mode I of crack opening.

Although this curve is not based on experimental data, it shows that at under 50% of RH there is not enough water for the initiation of the reactions. Significant expansions take place for RH greater than approximately 85%. We model these phenomena by a simple power function:

$$\varepsilon^{aar}/\varepsilon_{100} = H^m \quad (m = 8) \tag{8}$$

where H is the relative humidity and ε_{100} the free expansion at $H = 100\%$. The role of chemistry and humidity has been studied. At this point, the most important factor, from a structural point of view, has to be considered: the role of stress on the expansion.
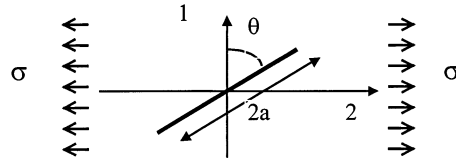
Relation Stress/Expansion

Uncoupling between kinetics and stress is considered. Shayan and Quick (4) have studied precasted and prestressed concrete railway sleepers deteriorated by AAR. Although they were prestressed in the longitudinal direction, these structures were cracked parallel to the prestress. Therefore, we can see that an applied stress can reduce, by a structural effect, the expansion in this direction but not in the perpendicular one. Considering this, we have tried to reproduce these observations by the use of fracture mechanics. What follows is a modeling of the expansion anisotropy, and in order to do that, some hypotheses have been made:

1. Cracks are considered to open only by Mode I, and cracks interactions are not taken into account (Fig. 5).
2. The free expansion ($_{[GRAPHIC]}$) is proportionnal to the volume of gel created by AAR (V_g), therefore, this involves a time t where structural expansions have started:

$$\varepsilon_0^{aar}(t) = \alpha_1 \cdot V_g(t) \tag{9}$$

3. The local pressures (σ_{eq}) developed by the swelling of the gel are proportionnal to the volume of gel created: the more the gel, the more the pressures are, and, according to the previous hypothesis, this leads to:

$$K_I = \sigma \cdot \sqrt{\pi a} \cdot \cos^2 \theta$$

FIG. 6.
Definition of the stress intensity factor.

$$\sigma_{eq}(t) = \alpha_2 \cdot V_g(t) = (\alpha_2/\alpha_1) \cdot \varepsilon_0^{aar}(t) = \beta \cdot \varepsilon_0^{aar}(t) \quad \beta = \alpha_2/\alpha_1 \tag{10}$$

Therefore, we consider that the local pressure developed by the gel is proportional to the only global variable we can measure: the free expansion. Expansions will be created by cracks opening which is controlled by fracture mechanics. In a bi-dimensional case, the stress intensity factor (K_I) is defined by Figure 6:

$$K_I = \sigma \cdot \sqrt{\pi a} \cdot \cos^2 \theta \tag{11}$$

where σ is the uniaxial applied stress, a is the half length of the crack, and θ the angle between the normal of the crack and the direction of the stress. If a linear elastic medium is considered, in a bi-dimensional case, the resulting stress intensity factor is a function of the two principal stresses and the pressure inside the crack, this leads to:

$$\begin{aligned} K_I &= \sqrt{\pi a} \cdot (\sigma_{eq}(t) + \sigma_1(t) \cdot \cos^2 \theta + \sigma_2(t) \cdot \sin^2 \theta) \\ &= \sqrt{\pi a} \cdot (\beta \cdot \varepsilon_0^{aar}(t) + \sigma_1(t) \cdot \cos^2 \theta + \sigma_2(t) \cdot \sin^2 \theta) \end{aligned} \tag{12}$$

The crack propagation, which is related to bulk deformation, thus the expansion, is controlled by a fracture mechanics statement: crack propagation occurs if the stress intensity factor is greater than the critical stress intensity factor (K_{IC}). Let $f(\theta,t)$ be the fraction of cracks that propagates at time t:

- if all the cracks are propagating $f(\theta,t) \rightarrow 1$;
- if no crack propagates $f(\theta,t) \rightarrow 0$;
- if $t \rightarrow \infty$ and $(\sigma1,\sigma2) \rightarrow 0$: $\varepsilon^{aar} \rightarrow \varepsilon_0^{aar}(\infty)$.

$\varepsilon^{aar}(\theta,t)$ is the strain at time t, in the direction θ, it is assumed that:

$$\varepsilon^{aar}(\theta,t) = \varepsilon_0^{aar}(\infty) \cdot f(\theta,t)/f(\theta,\infty) \tag{13}$$

First, we have to characterize the initial cracking. This can be done by an image analysis, for example, which provides informations about the initial cracking distribution as a mean value and a standard deviation of the half length of cracks. Rather than a, the variable α defined by $\alpha = \sqrt{\pi a}$ is used, and its mean value $\bar{\alpha}$ and standard deviation $\bar{\bar{\alpha}}$, which are deduced from the distribution of a (Fig. 7).

It is now necessary to join up $f(\theta,t)$, K_I, and the crack distribution. In the calculation of the probability of crack opening, α is transformed in a reduced centered normal value $B(\theta,t)$ by:
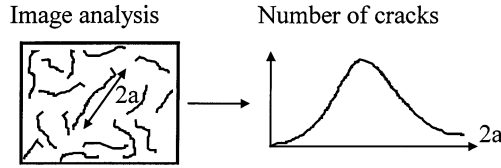
FIG. 7.
Quantification of the initial cracking.

$$B(\theta,t) = \frac{(K_{IC}/\beta \cdot \varepsilon_0^{aar}(t) + \sigma_1(t) \cdot \cos^2\theta + \sigma_2(t) \cdot \sin^2\theta) - \bar{\alpha}}{\bar{\bar{\alpha}}} \tag{14}$$

therefore, $f(\theta,t)$ is expressed by:

$$f(\theta,t) = \frac{1}{\sqrt{2\pi}} \int\limits_{-\infty}^{B(,t)} e^{(-\frac{u^2}{2})} \, du \tag{15}$$

Then, the expansion in the principal directions can be expressed by projection of the contribution of $\varepsilon^{aar}(\theta,t)$ for each θ in the principal strain axes. This leads to the expressions:

$$\varepsilon_1^{aar}(t) = \varepsilon_0^{aar}(\infty) \cdot \frac{\int_0^{\pi/2} f(\theta,t) \cdot \cos\theta \cdot d\theta}{\int_0^{\pi/2} f(\theta,\infty) \cdot \cos\theta \cdot d\theta} \tag{16}$$

$$\varepsilon_2^{aar}(t) = \varepsilon_0^{aar}(\infty) \cdot \frac{\int_0^{\pi.2} f(\theta,t) \cdot \sin\theta \cdot d\theta}{\int_0^{\pi/2} f(\theta,\infty) \cdot \sin\theta \cdot d\theta} \tag{17}$$

This work has been done for a two-dimensional problem but it can easily be extended to a three-dimensional one, considering an ellipsoidal inclusion for the crack and projection on the three axes. Here are some results coming from the model. In each case, we consider an applied load in one or two directions, in tension ($\sigma_i > 0$) or compression ($\sigma_i < 0$). The mechanical example is described in Figure 8.

The evolution of the probability of crack opening $f(\theta,t)$ is presented in Figure 9 at a given time. A high enough uniaxial compression prevents perpendicular cracks to this direction to open, but those which have a different angle contribute to the expansion.

The evolution of the two principal strains ε_1 and ε_2, in a uniaxial compression σ_1, is

FIG. 8.
Mechanical example.

Probability of crack opening - Direction 2

$\sigma_1 = 0$ MPa
$\sigma_2 = -5$ MPa

$f(\theta, t)$

Probability of crack opening - Direction 1
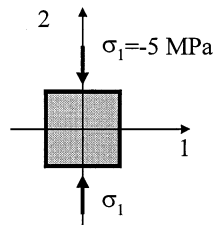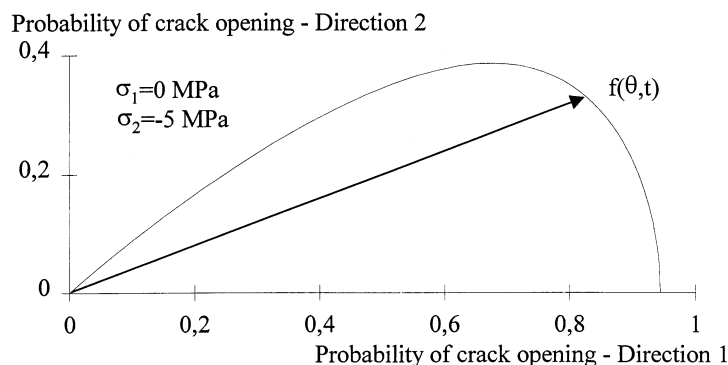
FIG. 9.

Representation of $f(\theta, t)$ in an uniaxial compression case.

presented Figure 10. There is a great reduction of the strain in the direction of the load, but in the perpendicular direction, the reduction is less important.

A compression load principally reduces the expansion in the direction of application, whereas a tension load principally increases the expansion in the same direction. Finally, this relatively simple way of describing the anisotropic expansion shows interesting results. Nevertheless, it is necessary to have an experimental validation. That is why, in the same time, some experiments on concrete bars with uniaxial applied stress have been started. This could provide some informations about the effect of an applied stress on the diminution of the expansion.

Numerical Simulations of AAR

The previous paragraphs allow us to bring to the fore the influence of the principal parameters of the AAR. At this point, in the aim of numerical simulations on a real structure, we have to take into account all the previous considerations. Then, the following equation for the evolution of the irreversible strains due to AAR may be proposed:

$$\varepsilon^{aar}(H, T, \sigma, t) = (H)^m \cdot \frac{\varepsilon_0}{A_0} \cdot (1 - A_0 - e^{-k_0 \cdot e^{-\frac{E_a}{RT} \cdot t}}) \cdot f(\sigma) \qquad (18)$$
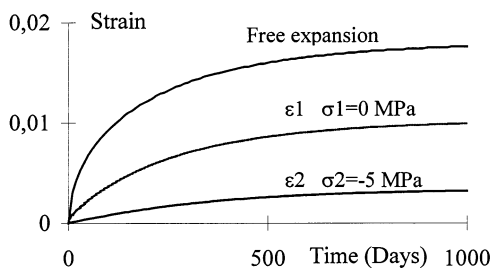
Strain

Free expansion

$\varepsilon 1$ $\sigma 1 = 0$ MPa

$\varepsilon 2$ $\sigma 2 = -5$ MPa

Time (Days)

FIG. 10.

Evolution of the free expansion, $\varepsilon 1$ and $\varepsilon 2$, in an uniaxial compression case, vs. time.
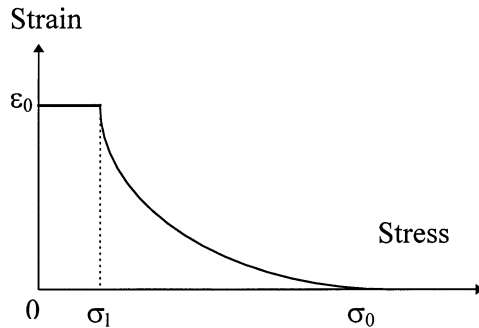
FIG. 11.
Decrease of expansion due to an applied stress (5).

where ε^{aar} and σ are respectively the strain tensor due to AAR and the stress tensor, $f(\sigma)$ is the relation between stresses and strains described in the previous paragraph. So, this function $\varepsilon^{aar}(H, T, \sigma, t)$ takes into account the principal parameters of AAR. An important point of this modeling is the decrease of expansion due to an applied stress. Some other models, based on the same principle, have been postulated. Charlwood et al. (5) have postulated a decrease of expansion only after a limit σ_λ ($\sigma l = 40$ psi $= 0, 28$ MPa), furthermore, expansions are stopped after a stress σ_0. This model is described in Figure 11.

This model is applied in the three directions of the space. It can be written as:

$$0 \leq \sigma \leq \sigma_1 \rightarrow \varepsilon^{aar} = \varepsilon_0 \tag{19}$$

$$\sigma_1 \leq \sigma \leq \sigma_0 \rightarrow \varepsilon^{aar} = K \cdot \log_{10}(\sigma/\sigma_0) \tag{20}$$

where $\varepsilon^{\alpha\alpha r}$ is the strain due to AAR; σ is the applied stress and ε_0 is the free expansion.

In order to compare the decrease of expansion given by the two models, we have computed the evolution of $\varepsilon^{\alpha\alpha r}(t)$ at a given time, with σ_λ varying from -10 MPa to 5 MPa and $\sigma_2 = 0$ MPa. The decrease of expansion for the principal strains vs. the uniaxial applied load is presented in Figure 12. A compressive load principally reduces the expansion in the direction of application, whereas a tension load principally increases the expansion in the same direction. Compared to the previous model, there is no sill of free expansion, what seems more realistic from a physical point of view.

So, $\varepsilon^{\alpha\alpha r}$, which is an inelastic and anisotropic part, will be coupled with a damageable concrete behaviour in attempting to provide numerical simulations. First, it will be necessary to make a thermal computation and one giving the repartition of the relative humidity H, in order to calculate $\varepsilon^{aar}(H, T, \sigma, t)$. This work is in progress on a dam case.

Conclusion

Until now, the alkali-aggregate reaction has brought about a lot of problems for engineers. It is difficult to take it into account with a good agreement towards reality because of the complexity of the phenomena. We have proposed here a new approach of modeling that takes into account some major parameters of the reactions. Such an approach is interesting from a theoretical point of view, because it allows us in a relatively simple way to model the
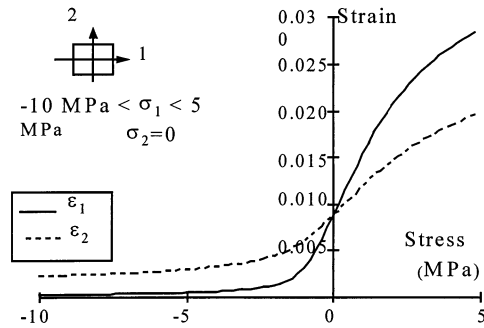
FIG. 12.
Evolution of the principal strains vs. principal stress σ_1.

anisotropy of the reaction. From a structural point of view, this anisotropy seems to be a very important parameter. Therefore, in order to make some simulations, this approach has to be validated by some experiments or in situ observations.

Acknowledgments

References

1. L.S. Dent Glasser and N. Kataoka, Proc. 5th ICAAR, Cape Town, S252/23, 1981.
2. S. Diamond, R.S. Barneyback, and L.J. Struble, Proc. 5th ICAAR, Cape Town, S252/22, 1981.
3. A.B. Poole, The Alkali-Silica Reaction in Concrete, R.N. Swamy (ed.), Blackie, London, 1992.
4. A. Shayan and G.W. Quick, ACI Mater. J. 89, 4 (1992).
5. R.G. Charlwood, R.R. Steele, Z.V. Solymar, and D.D. Curtis, Int. Conf. on AAR in Hydro-Electric Plants and Dams, CEA&CANCOLD, Fredericton, New Brunswick, Canada, 1992.